Published in final edited form as:
FEBS Lett. 2010 November 19; 584(22): 4500–4504. doi:10.1016/j.febslet.2010.10.024.

Leu628 of the KIX Domain of CBP is a Key Residue for the Interaction with the MLL Transactivation Domain

Munehito Arai[1,2,3], **H. Jane Dyson**[1], and **Peter E. Wright**[1,*]

[1] Department of Molecular Biology and Skaggs Institute for Chemical Biology, The Scripps Research Institute, 10550 North Torrey Pines Road, La Jolla, California 92037

[2] Protein Design Research Group, Institute for Biological Resources and Functions, National Institute of Advanced Industrial Science and Technology (AIST), 1-1-1 Higashi, Tsukuba, Ibaraki 305-8566, Japan

[3] Department of Life Sciences, Graduate School of Arts and Sciences, The University of Tokyo, 3-8-1 Komaba, Meguro-ku, Tokyo 153-8902, Japan

Abstract

Physical interaction between the transactivation domain (TAD) of the mixed-lineage leukemia protein (MLL) and the KIX domain of the CREB binding protein (CBP) is necessary for MLL-mediated transcriptional activation. We show by alanine-scanning mutagenesis that hydrophobic surface residues of KIX, especially L628, are energetically important for binding the MLL TAD. NMR studies of the KIX-L628A mutant suggest that L628 plays a crucial role in conformational transitions at the MLL binding site, necessary for high affinity interactions with MLL. Unexpectedly, MLL also binds to the c-Myb/pKID site of KIX, highlighting the complex nature of interactions involving intrinsically disordered transcriptional activators.

Keywords

protein-protein interaction; NMR chemical shift perturbation; mixed lineage leukemia; transcriptional coacvitator CBP; transactivation domain; isothermal titration calorimetry

1. Introduction

Gene activation in higher eukaryotes is accomplished through the concerted action of transcription factors and transcriptional coactivators [1]. CBP/p300 are general transcriptional coactivators that recruit the basal transcription machinery and modify chromatin via their histone acetyltransferase activities [2]. They contain modular protein binding domains, including the KIX domain, that physically interact with various transcription factors [3]. The KIX domain provides two distinct binding surfaces for

[*]Corresponding author: wright@scripps.edu, Phone: 858-784-9721; Fax: 858-784-9822.

Structured summary:
MINT-8044564, MINT-8044580, MINT-8044598, MINT-8044616, MINT-8044634, MINT-8044656:
Cbp (uniprotkb:P45481) and *MLL* (uniprotkb:Q03164) *bind* (MI:0407) by *isothermal titration calorimetry* (MI:0065)
MINT-8044696:
Cbp (uniprotkb:P45481) and *MLL* (uniprotkb:Q03164) *bind* (MI:0407) by *nuclear magnetic resonance* (MI:0077)

interactions with transcription factors; the TADs of the phosphorylated kinase-inducible domain of CREB (pKID) and c-Myb bind to a hydrophobic groove formed by the first and third α-helices of KIX, while the TAD of MLL binds to an opposite surface of KIX from the c-Myb/pKID site (Fig. 1A) [4–6].

MLL belongs to the evolutionarily conserved trxG family, which acts as a positive regulator of homeobox (Hox) gene expression to control segment specificity in early embryogenesis through an epigenetic mechanism [7]. Physical interaction between the MLL TAD and KIX is necessary for MLL-mediated transcriptional activation [8]. Indeed, chromosomal translocations involving MLL cause the loss of several MLL domains including the TAD, resulting in infant and treatment-related leukemias [7]. The NMR structure of the ternary KIX·MLL·c-Myb complex revealed that the MLL TAD binds to a groove formed at the interface between the G_2 3_{10}-helix and the second and third α-helices of KIX [6]. However, it is not clear which residues of KIX are energetically important in MLL binding. Here, we show by alanine-scanning mutagenesis and NMR experiments that L628 of KIX is a key residue for the interaction with the MLL TAD.

2. Materials and Methods

2.1. Sample preparation

Wild-type and mutant KIX domains (residues 586-672) of mouse CBP were constructed, expressed and purified as previously described [4,9]. Both wild-type and L628A mutant KIX were prepared with [^{15}N]- and [^{15}N, ^{13}C]-labeling for NMR experiments. Human MLL (2842-2469) was produced and purified as described [9]. An additional glycine residue was present at the N-terminus of MLL as a remnant following thrombin cleavage. The molecular weights of the proteins were confirmed by mass spectrometry. The MLL concentration was measured using the Pierce BCA protein assay kit. The KIX concentration was determined by absorbance at 280 nm.

2.2. Isothermal titration calorimetry (ITC)

ITC experiments were performed at 30°C using a MicroCal Omega VP-ITC instrument (MicroCal, Amherst, MA) as previously described [5,10]. Samples were prepared in 20 mM Tris/acetate (pH 7.0) and 50 mM NaCl. All experiments were performed in duplicate. See Supplementary text for details.

2.3. Circular dichroism (CD) spectra

CD spectra were measured on an Aviv 62DS spectropolarimeter at 30°C. The urea-induced equilibrium unfolding transition of KIX was monitored at 222 nm by preparing separate samples at each urea concentration. The mean residue ellipticity (MRE) was calculated as described [11]. The equilibrium unfolding transition curves were analyzed assuming a two-state transition [11].

2.4. NMR spectroscopy

NMR spectra were recorded using Bruker 500, 600, and 800 MHz spectrometers in buffer containing 20 mM d_{11}-Tris/d_4-acetate (pH 7.0), 50 mM NaCl, 0.2% (w/v) NaN_3 and 10% ^2H_2O at 30°C, and analyzed using NMRPipe [12] and NMRView [13]. Backbone resonances of the wild-type and the L628A mutant of KIX in the free and the MLL-bound forms were assigned by standard triple resonance experiments using HNCA [14], HN(CO)CA [15], HNCACB [16], and CBCA(CO)NH [14]. The typical protein concentration was 0.5 mM. In titration experiments, an aliquot of ~2 mM unlabeled MLL was added to the NMR tube containing ^{15}N-labeled KIX at each titration step.

2.5. Dissociation constants from chemical shift titrations

The dissociation constants and the binding sites for the primary and secondary MLL binding to KIX were estimated by a global fit of ^{1}H and ^{15}N chemical shift changes, assuming a two-site binding model [10,17]. Singular value decomposition (SVD) was used to estimate the number of binding sites and to remove the contribution of noise to experimental data [11,18] (MA, JC Ferreon, HJD, and PEW, manuscript in preparation). See Supplementary text for details.

3. Results & Discussion

3.1. Ala-scanning mutagenesis at the MLL binding site

We introduced single-site Ala substitutions at F612, R624, L628, Y631, L664, and R668 of KIX, residues which have direct contacts with MLL in the ternary complex [6]. The six mutants showed essentially the same far-UV CD spectra, indicating that overall secondary structure is unaffected by the mutations (Fig. 1B). However, the Y631A mutant was destabilized to urea unfolding, while the L628A mutant was slightly stabilized (Fig. 1C and Supplementary Table S1).

The equilibrium dissociation constant, K_d, for MLL binding measured by ITC was 2.1 μM for wild-type KIX, consistent with the K_d of 2.8 μM reported previously for a shorter MLL construct [5] (Fig. 1D,Supplementary Table S1 and Supplementary Fig. S1). However, K_d was greatly affected by the mutations, with a reduction of over an order of magnitude in affinity seen for Y631A, L664A and F612A, and was too large to be determined for L628A. Lesser reductions of affinity were seen for R624A and R668A, indicating that hydrophobic residues are energetically more important for the KIX·MLL interaction. Consistent with this conclusion, Y631, L664, F612 and L628 are in contact with hydrophobic residues I2849, F2852, V2853, and L2854 of MLL [8].

3.2. The KIX-L628A mutant

Strikingly, MLL binding by the KIX-L628A mutant was not observed by ITC. We therefore performed an HSQC titration in which unlabeled MLL was added stepwise into ^{15}N-labeled KIX-L628A (Fig. 2A and Supplementary Fig. S2). Upon titration with MLL, the KIX-L628A cross-peaks showed fast-exchanging shifts with a curvature, indicating weak but detectable interactions at more than one site. This was confirmed by SVD analysis, which gives an estimate of the number of meaningful components necessary for explaining the observed data set [11,18] (Supplementary Fig. S3). The titration points were therefore globally fit using a two-site binding model (Fig. 2B and Supplementary Fig. S4), giving a dissociation constant for the primary binding, K_{d1}, of 220 (±10) μM. The primary MLL binding site of KIX-L628A was found to be very similar to that of the wild-type KIX (Fig. 2C and Supplementary Fig. S5).

Average ^{1}H and ^{15}N chemical shift differences, $\Delta\delta(N,H)_{av}$, between the wild-type and the L628A mutant of KIX in the free form showed that F612 and V629, which both contact L628A, are greatly perturbed by the mutation (Fig. 3A). Interestingly, T614, which does not have direct contact with L628, shows a very large chemical shift perturbation, indicating that through F612, the L628A mutation perturbs the L_{12} loop located between the α_1 and α_2 helices. However, secondary Cα shifts (Fig. 3A, lower panel) indicate that the overall secondary structures are not perturbed by the mutation.

Binding of MLL to wild-type KIX induces enhanced formation of the G_2 3_{10}-helix and displacement of the L_{12} loop, allowing the side-chain of F612 to make close hydrophobic contacts with MLL (Fig. 3B-D) [5]. However, such a helix enhancement was not observed

in KIX-L628A (Fig. 3B). These results suggest that in addition to hydrophobic contacts with MLL, L628 may play crucial roles in the L_{12} loop displacement and the enhanced G_2 helix formation, which are necessary for high affinity binding with MLL.

3.3. Secondary MLL binding to KIX

Unexpectedly, HSQC titrations also showed the presence of secondary MLL binding to KIX-L628A, with a dissociation constant, K_{d2}, of 1.63 (±0.05) mM (Fig. 2). Large chemical shift changes were observed in and around the c-Myb/pKID binding site upon secondary binding, indicating that the second MLL ligand binds very weakly to the c-Myb/pKID site (Fig. 2D). Chemical shift perturbations due to binding in the secondary site were also observed at the primary MLL site (Fig. 2D). This is probably due to conformational changes rather than direct binding, because it is unlikely that two MLL molecules can bind simultaneously in the same site on KIX. Alternatively, it might be possible that deconvolution of the chemical shift changes associated with primary and secondary binding events was not perfect, because both binding events are not clearly separated in the titration curves, compared, for example, with ^{15}N-TAZ2 titration with p53 [17].

The secondary MLL binding to the c-Myb/pKID site was confirmed by HSQC titration of ^{15}N-labeled wild-type KIX with MLL (Fig. 4A and Supplementary Figure S6). Whereas slow to intermediate exchange was observed below 1:1 KIX:MLL ratios due to primary binding, fast-exchanging shifts were observed at greater than 1:1 ratios, indicating the presence of secondary MLL binding, which was confirmed by SVD analysis (Supplementary Fig. S7). The titration curves referenced to the data at a 1:1 KIX:MLL ratio were globally fit with a two-site binding model, assuming that K_{d1} = 2.1 μM and that the chemical shift changes in the primary binding site are zero (Fig. 4B and Supplementary Fig. S8). The analysis revealed large chemical shift perturbations in and around the c-Myb/pKID binding site with a K_{d2} of 920 (±20) μM (Fig. 4C,D and Supplementary Fig. S9), showing unequivocally that MLL binds KIX at two sites.

MLL has an amphipathic φ-x-x-φ-φ motif (φ = bulky hydrophobic residue and x = any residue), which is conserved in many KIX binding proteins including c-Myb and pKID [10]. The primary sequence similarity indicates that MLL has the potential to bind the c-Myb/pKID site through the amphipathic motif, supporting our present finding. Although the affinity of the secondary binding event is weak, it highlights the complex nature of interactions involving hub proteins such as transcriptional coactivators.

Supplementary Material

Refer to Web version on PubMed Central for supplementary material.

Acknowledgments

This work is supported by grant CA96865 from the National Institutes of Health and the Skaggs Institute for Chemical Biology. M.A. was supported in part by Grant-in-Aid for Scientific Research on Innovation Areas from MEXT, Japan.

Abbreviations

CD	circular dichroism
CBP	CREB binding protein
CREB	cyclic-AMP response element binding protein

HSQC	heteronuclear single quantum correlation
ITC	isothermal titration calorimetry
MLL	mixed-lineage leukemia protein
MRE	mean residue ellipticity
pKID	phosphorylated kinase-inducible domain of CREB
SD	standard deviation
SVD	singular value decomposition
TAD	transactivation domain

References

1. Spiegelman BM, Heinrich R. Biological control through regulated transcriptional coactivators. Cell. 2004; 119:157–167. [PubMed: 15479634]
2. Goodman RH, Smolik S. CBP/p300 in cell growth, transformation, and development. Genes Dev. 2000; 14:1553–1577. [PubMed: 10887150]
3. Dyson HJ, Wright PE. Intrinsically unstructured proteins and their functions. Nat Rev Mol Cell Biol. 2005; 6:197–208. [PubMed: 15738986]
4. Radhakrishnan I, Perez-Alvarado GC, Parker D, Dyson HJ, Montminy MR, Wright PE. Solution structure of the KIX domain of CBP bound to the transactivation domain of CREB: a model for activator:coactivator interactions. Cell. 1997; 91:741–752. [PubMed: 9413984]
5. Goto NK, Zor T, Martinez-Yamout M, Dyson HJ, Wright PE. Cooperativity in transcription factor binding to the coactivator CREB-binding protein (CBP). The mixed lineage leukemia protein (MLL) activation domain binds to an allosteric site on the KIX domain. J Biol Chem. 2002; 277:43168–43174. [PubMed: 12205094]
6. De Guzman RN, Goto NK, Dyson HJ, Wright PE. Structural basis for cooperative transcription factor binding to the CBP coactivator. J Mol Biol. 2006; 355:1005–1013. [PubMed: 16253272]
7. Popovic R, Zeleznik-Le NJ. MLL: how complex does it get? J Cell Biochem. 2005; 95:234–242. [PubMed: 15779005]
8. Ernst P, Wang J, Huang M, Goodman RH, Korsmeyer SJ. MLL and CREB bind cooperatively to the nuclear coactivator CREB-binding protein. Mol Cell Biol. 2001; 21:2249–2258. [PubMed: 11259575]
9. Sugase K, Landes MA, Wright PE, Martinez-Yamout M. Overexpression of post-translationally modified peptides in *Escherichia coli* by co-expression with modifying enzymes. Protein Expr Purif. 2008; 57:108–115. [PubMed: 18054500]
10. Lee CW, Arai M, Martinez-Yamout MA, Dyson HJ, Wright PE. Mapping the interactions of the p53 transactivation domain with the KIX domain of CBP. Biochemistry. 2009; 48:2115–2124. [PubMed: 19220000]
11. Arai M, Iwakura M. Probing the interactions between the folding elements early in the folding of *Escherichia coli* dihydrofolate reductase by systematic sequence perturbation analysis. J Mol Biol. 2005; 347:337–353. [PubMed: 15740745]
12. Delaglio F, Grzesiek S, Vuister GW, Zhu G, Pfeifer J, Bax A. NMRPipe: a multidimensional spectral processing system based on UNIX pipes. J Biomol NMR. 1995; 6:277–293. [PubMed: 8520220]
13. Johnson BA, Blevins RA. NMR View - a computer-program for the visualization and analysis of NMR data. J Biomol NMR. 1994; 4:603–614.
14. Grzesiek S, Bax A. Improved 3D triple-resonance NMR techniques applied to a 31-kkDa protein. J Magn Reson. 1992; 96:432–440.

15. Bax A, Ikura M. An efficient 3D NMR technique for correlating the proton and ^{15}N backbone amide resonances with the α-carbon of the preceding residue in uniformly ^{15}N/^{13}C enriched proteins. J Biomol NMR. 1991; 1:99–104. [PubMed: 1668719]

16. Wittekind M, Mueller L. HNCACB, a high-sensitivity 3D NMR experiment to correlate amide-proton and nitrogen resonances with the α-carbon and β-carbon resonances in proteins. J Magn Reson. 1993; 101:201–205.

17. Ferreon JC, Lee CW, Arai M, Martinez-Yamout MA, Dyson HJ, Wright PE. Cooperative regulation of p53 by modulation of ternary complex formation with CBP/p300 and HDM2. Proc Natl Acad Sci USA. 2009; 106:6591–6596. [PubMed: 19357310]

18. Henry ER, Hofrichter J. Singular value decomposition - application to analysis of experimental data. Methods Enzymol. 1992; 210:129–192.

19. Koradi R, Billeter M, Wuthrich K. MOLMOL: a program for display and analysis of macromolecular structures. J Mol Graph. 1996; 14:51–55. 29–32. [PubMed: 8744573]

20. Wishart DS, Bigam CG, Holm A, Hodges RS, Sykes BD. ^{1}H, ^{13}C and ^{15}N random coil NMR chemical shifts of the common amino acids. I. Investigations of nearest-neighbor effects. J Biomol NMR. 1995; 5:67–81. [PubMed: 7881273]

21. Zor T, De Guzman RN, Dyson HJ, Wright PE. Solution structure of the KIX domain of CBP bound to the transactivation domain of c-Myb. J Mol Biol. 2004; 337:521–534. [PubMed: 15019774]

Appendix A. Supplementary Data

Supplementary data associated with this article can be found in the online version.

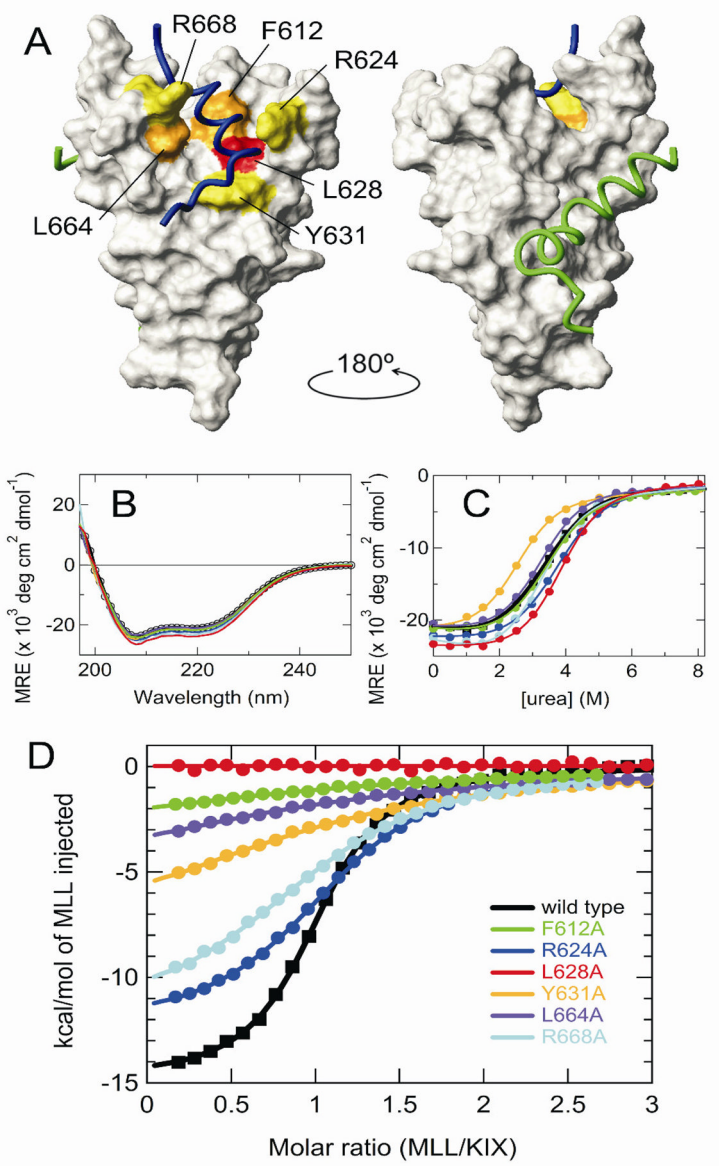

Figure 1.

(A) Representation of the KIX structure in the ternary KIX·MLL·c-Myb complex (PDB 2AGH [6]). The six mutation sites are mapped onto the surface of KIX, color coded to indicate the effect of Ala substitution on K_d for MLL binding: yellow, 2-15× increase in K_d; orange, 25-40× increase; red, 100× increase. Backbones of the bound MLL (2842-2860 only) and c-Myb are shown in blue and green, respectively. The figure was prepared using MOLMOL [19]. (B) Far-UV CD spectra, (C) urea-induced equilibrium unfolding transition, and (D) MLL binding isotherms of the wild-type and mutant KIX. Color codes are shown in (D). In (C) and (D), continuous lines are the curves fitted to a two-state transition and a one-site binding model, respectively.

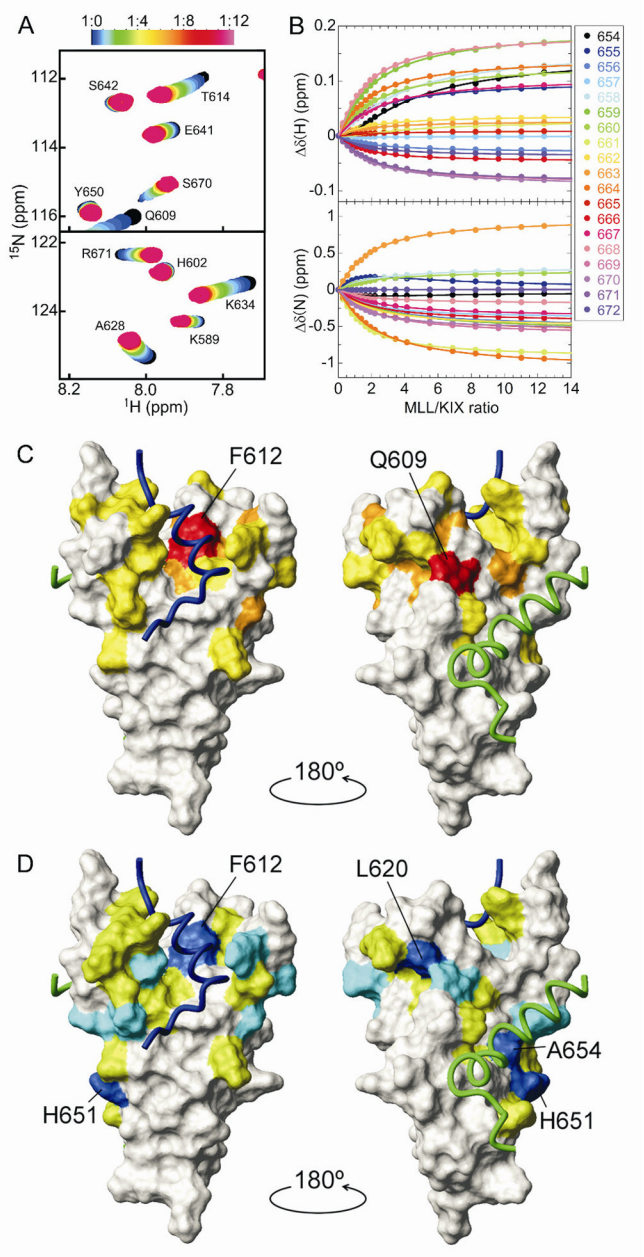

Figure 2.

(A) Regions of the ^{1}H-^{15}N HSQC spectrum of the KIX-L628A mutant showing chemical shift changes upon titration with MLL. The cross-peak color changes gradually from black (free) to magenta according to the concentration ratio as shown in the bar above the figure. (B) ^{1}H and ^{15}N chemical shift titration curves for a subset of KIX-L628A resonances (colored points corresponding to residues according to the legend) upon titration with increasing amounts of MLL. The lines represent a global fit to the titration data, using a two-site binding model with K_{d1} = 220 μM and K_{d2} = 1.63 mM. (C,D) MLL binding sites on KIX-L628A. The weighted average chemical shift differences

$[\Delta\delta(\mathrm{N,H})_{av} = \sqrt{(\Delta\delta_{H})^2+(\Delta\delta_{N}/5)^2}]$ for KIX-L628A amide resonances between the free form and the bound form, in which the primary (C) or secondary binding site (D) is occupied, are

mapped onto the surface of KIX in the ternary complex, using colors to indicate changes in chemical shift greater than 2 × standard deviation (SD) from the mean (red and blue), between 1 and 2 × SD from the mean (orange and cyan), and between mean and 1 × SD from the mean (yellow and green).

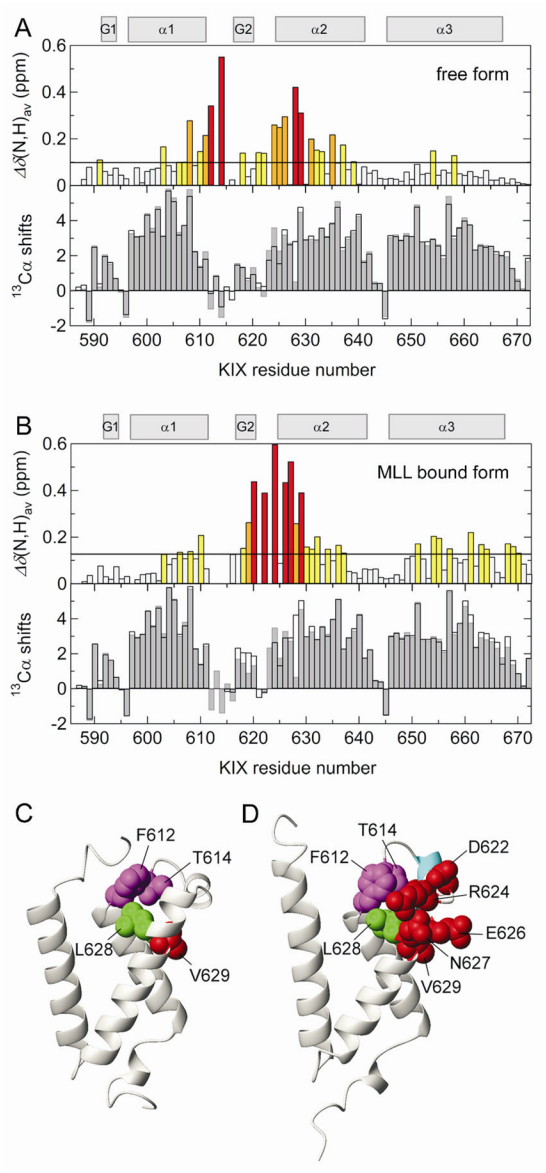

Figure 3.

(A, upper) Histogram showing $\Delta\delta(N,H)_{av}$ between the wild-type and the L628A mutant of KIX in the free form. Color codes are the same as in Fig. 2. (A, lower) Histogram showing the secondary $^{13}C\alpha$ chemical shifts calculated by subtraction of random coil values [20] from the experimental data for the wild-type KIX (open bars) and the L628A mutant (gray bars) in the free form. Regions showing positive secondary Cα chemical shifts indicate a helical conformation. Secondary structure elements in the ternary KIX·MLL·c-Myb complex [6] are depicted at the top. (B) The same as in (A), but in the presence of MLL (1:1 and 1:2 KIX:MLL ratios for the wild-type KIX and the L628A mutant, where 94% and 74% of KIX are in the MLL-bound form, respectively). (C,D) The KIX structures in the binary KIX·c-Myb complex (PDB 1SB0 [21]) and in the ternary KIX·MLL·c-Myb complex, respectively. Residues having large $\Delta\delta(N,H)_{av}$ are shown by spheres of radius corresponding to the van der Waals radius of each atom. In (D), the G_2 helix is colored cyan.

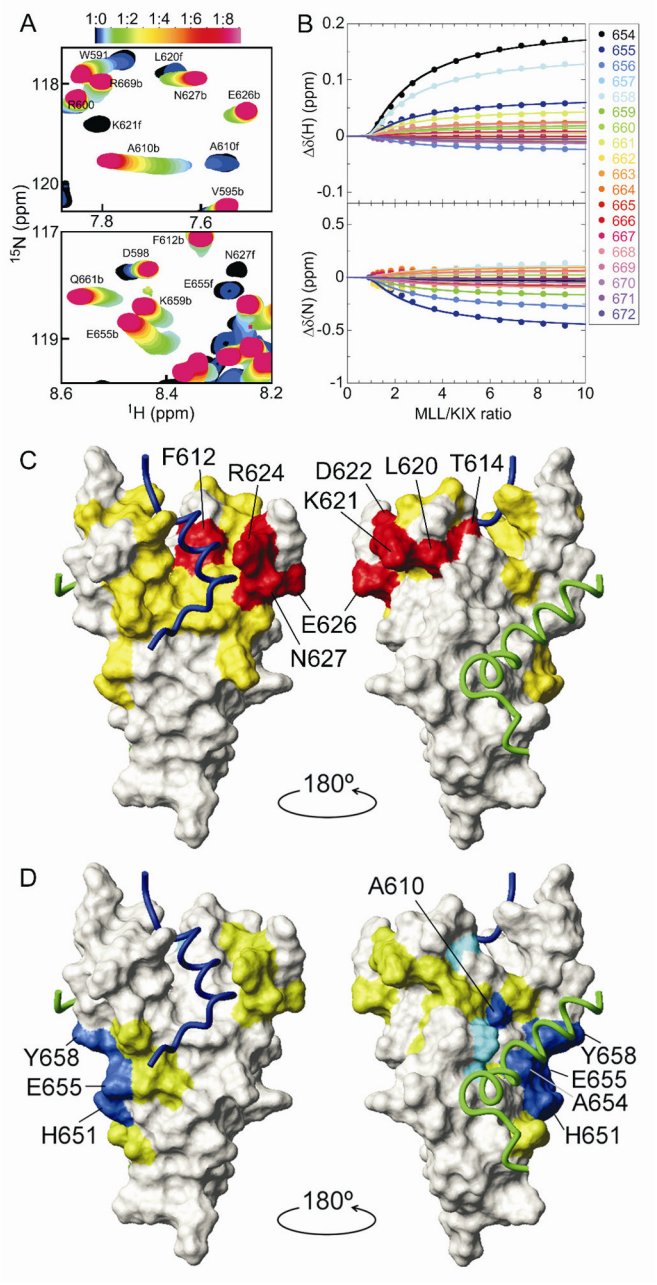

Figure 4.

(A) Regions of the ^{1}H-^{15}N HSQC spectrum of wild-type KIX showing chemical shift changes upon titration with MLL. b and f indicate the peaks for the bound and free forms, respectively. (B) ^{1}H and ^{15}N chemical shift titration curves for a subset of KIX resonances upon titration with increasing amounts of MLL. The lines represent a global fit to the titration data, using a two-site binding model with K_{d1} = 2.14 μM and K_{d2} = 920 μM. (C,D) MLL binding sites on the wild-type KIX, as shown in Fig. 2C,D. $\Delta\delta(N,H)_{av}$ for primary binding was obtained from the HSQC spectra at 1:0 and 1:1 KIX:MLL ratios. $\Delta\delta(N,H)_{av}$ for secondary binding was obtained from a global fit of titration curves.